Microwave dielectric relaxation in cubic bismuth based pyrochlores containing titanium

Hong Wang[a)]
Electronic Materials Research Laboratory, Key Laboratory of the Ministry of the Education, Xi'an Jiaotong University, Xi'an 710049, China

Stanislav Kamba[b)]
Institute of Physics, ASCR, Na Slovance 2, 18221 Prague 8, Czech Republic

Huiling Du and Meiling Zhang
Electronic Materials Research Laboratory, Key Laboratory of the Ministry of the Education, Xi'an Jiaotong University, Xi'an 710049, China

Chih-Ta Chia
Department of Physics, National Taiwan Normal University, Taipei 116, Taiwan

S. Veljko, S. Denisov, F. Kadlec, and Jan Petzelt
Institute of Physics, ASCR, Na Slovance 2, 18221 Prague 8, Czech Republic

Xi Yao
Electronic Materials Research Laboratory, Key Laboratory of the Ministry of the Education, Xi'an Jiaotong University, Xi'an 710049, China

(Received 6 January 2006; accepted 18 April 2006; published online 7 July 2006)

Cubic pyrochlore $(Bi_{1.5}Zn_{0.5})(Zn_{0.5-x/3}Ti_xNb_{1.5-2x/3})O_7$ ceramics with $0 \leqslant x \leqslant 1.5$ were synthesized and investigated between 100 Hz and 100 THz by means of broadband dielectric spectroscopy, time-domain terahertz transmission spectroscopy, Fourier transform infrared reflectivity spectroscopy and Raman scattering. $Bi_{1.5}ZnNb_{1.5}O_7$ exhibits a microwave dielectric relaxation which slows down and broadens remarkably on cooling. Careful structural investigations confirmed that the relaxation originates in hopping of disordered Bi and part of Zn atoms in the *A* sites of the pyrochlore structure. Substitution of Ti atoms to the *B* sites, i.e., increasing *x*, results in an increase of the microwave permittivity from 150 to 200 of the relaxation frequency and also of the microwave quality *Q*. Low temperature Raman scattering experiments did not reveal any phase transition in the samples under study. © *2006 American Institute of Physics*.
[DOI: 10.1063/1.2208915]

I. INTRODUCTION

With the recent development of low temperature cofiring ceramic (LTCC) devices, the demands for materials that can be cofired with metal electrodes and other ceramics have been increasing in the past decade.

$Bi_2O_3-ZnO-Nb_2O_5$ (BZN) based pyrochlore ceramics were first explored by Chinese engineers in 1970s for multilayer capacitors.[1] Recently, they attracted more attention due to their excellent dielectric properties and lower firing temperatures as promising candidates for LTCC and microwave (MW) passive components. Stoichiometric pyrochlores have the general formula $A_2B_2O_7$. The structure is composed of two interpenetrated networks: BO_6 octahedra with shared vertices form a three-dimensional network resulting in large cavities which contain the O′ and *A* atoms in an A_2O' tetrahedral net. The structure can accommodate a wide range of different chemical substituents and defect structures also exist. In bismuth based pyrochlore systems, the general chemical formula can be written as $(Bi_{3x}Zn_{2-3x})\times(Zn_xNb_{2-x})O_7$. For $x=0.5$, the chemical formula is $Bi_{1.5}ZnNb_{1.5}O_7$ and the system crystallizes in cubic pyrochlore structure.[2,3] The ceramics has a MW permittivity of about 150, quality factor times frequency $Q\times f\sim 100$ GHz, and a temperature coefficient of capacitance (TCC) about −400 ppm/°C.[4,5] For $x=2/3$, the chemical formula is $Bi_2Zn_{2/3}Nb_{4/3}O_7$, structure is monoclinic, permittivity about 80, $Q\times f\sim 3000$ GHz, and TCC $\sim +200$ ppm/°C.[5,6] Two-phase ceramics with appropriate compositions achieve TCC close to zero with permittivity ~100 and $Q\sim f\sim 300$ GHz.[7]

The high dielectric constants, relatively low dielectric losses (high quality factor), controllable TCC with the low sintering temperatures (below 1000 °C), and high tunability with electric field[8–10] make this system a very appealing candidate for applications in low-fire high-frequency multilayer devices. Many works were carried out on the formation, stability, and crystallographic characterization of this system as well as successful manufacturing of prototype devices including LC filters and LTCC systems.[11–14] Very recently, a field-effect transistor was fabricated with transparent oxide semiconductor ZnO and high permittivity $Bi_{1.5}ZnNb_{1.5}O_7$ as the gate insulator.[15] The devices exhibited very low operation voltages (<4 V) due to the high capacity of the BZN dielec-

[a)]Electronic mail: hwang@mail.xjtu.edu.cn
[b)]Electronic mail: kamba@fzu.cz

tric. This together with a high optic transparency makes this device very promising for transparent electronics.

A low temperature dielectric anomaly in bismuth based cubic pyrochlores was first observed by Cai *et al.*[16] and then it was studied by Cann *et al.*[17] who stated that the anomaly appears similar to the dispersion that occurs near the freezing temperature of dipolar glass systems. A wide-range dielectric response of the cubic pyrochlore $Bi_{1.5}ZnNb_{1.5}O_7$ and zirconolitelike pyrochlore phase $Bi_2Zn_{2/3}Nb_{4/3}O_7$ was studied by Kamba *et al.*[18] and Petzelt and Kamba.[19] They showed that no dielectric relaxation exists in $Bi_2Zn_{2/3}Nb_{4/3}O_7$ below phonon frequencies because of the ordered crystal structure, while in the case of $Bi_{1.5}ZnNb_{1.5}O_7$ a strong relaxation arises as a consequence of the local hopping of atoms in the *A* and O′ positions of the pyrochlore structure among several local potential minima. The inhomogeneous distribution of Zn atoms between *A* and *B* sites gives rise to random fields and nonperiodic interatomic potential, which accounts for the anomalous broad distribution of dielectric relaxations at low temperatures in cubic BZN.[18]

The structure and low-frequency (<1 MHz) dielectric properties of cubic BZN doped with titanium were studied by Cai *et al.*[16] and Valant and Davies.[20,21] They found that the permittivity increases with Ti content up to 200 and the dielectric loss remains low ($\tan\delta < 10^{-4}$) at 1 MHz. Du and Yao[22,23] investigated dielectric properties of $(Bi_{1.5}Zn_{0.5})\times(Zn_{0.5-x/3}Ti_xNb_{1.5-2x/3})O_7$ ceramics with $0 \leqslant x \leqslant 1.5$ below 1 MHz down to 100 K and they observed a dielectric anomaly similar to $Bi_{1.5}ZnNb_{1.5}O_7$. The anomaly shifts systematically to lower temperatures with increasing Ti content.

The aim of this paper is to extend the study of the dielectric relaxation in $(Bi_{1.5}Zn_{0.5})(Zn_{0.5-x/3}Ti_xNb_{1.5-2x/3})O_7$ $(0 \leqslant x \leqslant 1.5)$ ceramics to MW, terahertz, and infrared (IR) frequency ranges and to combine it with a detailed structural investigation.

II. EXPERIMENT

The ceramic samples were prepared by conventional mix-oxide method. Raw materials Bi_2O_3, ZnO, Nb_2O_5, and TiO_2 were used as starting materials and weighed according to the composition $(Bi_{1.5}Zn_{0.5})(Zn_{0.5-x/3}TixNb_{1.5-2x/3})O_7$, with *x* equal to 0, 0.25, 0.5, 1.0, and 1.5. The weighed batches were wet milled in a planetary ball mill for 4 h. The slurry was then dried and calcined at 700–800 °C for 2 h. The calcined powders were ball milled again, dried, and pressed into disks and cylinder samples. The samples were sintered from 960–1100 °C for 2 h in air. The higher the Ti contents, the higher the sintering temperature.

The density of the samples was measured by the Archimedes method. Silver electrodes were used for dielectric measurement. X-ray diffraction (XRD) (Rigaku, Cu $K\alpha$ radiation) was carried out for the sintered samples at room temperature and the lattice parameter was calculated precisely.

Dielectric measurements in the frequency range of 1 MHz–1.8 GHz were performed by an HP 4291B impedance analyzer with a NOVOCONTROL BDS 2100 coaxial sample cell and a SIGMA SYSTEM M18 temperature chamber (operation range of 100–570 K). The dielectric parameters were calculated taking into account the electromagnetic field distribution in the samples. The microwave dielectric properties at room temperature were measured by putting the cylindrical samples in a $TE_{01\delta}$ cylindrical resonant cavity with an 8720ES network analyzer at approximately 2 ~3 GHz for measuring the $TE_{01\delta}$ modes. The temperature coefficient of resonance frequency τ_f was measured using the same method connected with a Delta 9023 temperature chamber.

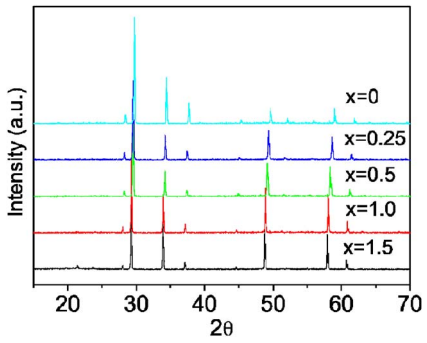

FIG. 1. (Color online) XRD patterns of $(Bi_{1.5}Zn_{0.5})\times(Zn_{0.5-x/3}Ti_xNb_{1.5-2x/3})O_7$ ceramics.

Measurements at terahertz frequencies were performed in the transmission mode using an amplified femtosecond laser system. Two [110] ZnTe crystal plates (1 mm thick) were used to generate (by optical rectification) and detect (by electro-optic sampling) the terahertz pulses. Our terahertz technique allows determining the complex dielectric response, $\varepsilon^*(\omega)=\varepsilon'(\omega)-i\varepsilon''(\omega)$, in the range from 3 to 80 cm^{-1} (0.1–2.4 THz). The actual spectral range depends on the transparency of the samples investigated and can be also influenced by sample thickness. In our case a thickness of 353 μm was used.

IR reflectivity spectra at room temperature were obtained using a Fourier transform spectrometer Bruker IFS 113v in the frequency range of 30–3000 cm^{-1} (0.9–90 THz). The reflectivity spectra, together with the complex permittivity $\varepsilon^*(\omega)$ spectra obtained from the terahertz measurements, were fitted using a sum of damped harmonic oscillators,

$$\varepsilon^*(\omega) = \sum_{j=1}^{n} \frac{\Delta\varepsilon_j \omega_j^2}{\omega_j^2 - \omega^2 + i\omega\gamma_j} + \varepsilon_\infty, \tag{1}$$

where $\varepsilon^*(\omega)$ is related to reflectivity $R(\omega)$ by

$$R(\omega) = \left| \frac{\sqrt{\varepsilon^*(\omega)} - 1}{\sqrt{\varepsilon^*(\omega)} + 1} \right|^2, \tag{2}$$

where ω_j, γ_j, and $\Delta\varepsilon_j$ are the frequency, damping, and dielectric strength of the *j*th mode, respectively. The high-frequency permittivity ε_∞ results from electronic absorption processes much above the phonon frequencies (typically in UV-VIS range).

A DILOR XY 800 triple grating Raman spectrometer equipped with a liquid-nitrogen-cooled charge-coupled device (CCD) detector was used for temperature-dependent Raman measurements. The 514.5 nm line of an Ar^+ laser with

TABLE I. Microwave dielectric properties of $(Bi_{1.5}Zn_{0.5})\times(Zn_{0.5-x/3}Ti_xNb_{1.5-2x/3})O_7$ ceramics.

x	ε'	Q	f (GHz)	Lattice parameter (Å)	τ_f (ppm/°C)	Density (g/cm^3)
0	149.8	38	2.3898	10.5524	+191	7.120
0.25	150.2	29	2.6850	10.5174	+218	7.073
0.5	158.6	66	2.5201	10.4867	+280	6.980
1.0	180.5	57	2.3551	10.4183	+400	6.885
1.5	201.2	67	2.2760	10.3586	+518	6.777

an output power of 200 mW was used for excitation and a 90° scattering geometry was employed. The samples were placed in a closed cycle cryogenic refrigerator and were cooled down to 10 K. The Raman spectra were recorded with a resolution of approximately 0.5–1 cm^{-1}.

III. RESULTS AND DISCUSSIONS

The XRD patterns of $(Bi_{1.5}Zn_{0.5})\times(Zn_{0.5-x/3}Ti_xNb_{1.5-2x/3})O_7$ samples are shown in Fig. 1. The structure of all samples is cubic pyrochlore[5] (PDF54-971) with the lattice parameter decreasing linearly from 10.5524 to 10.3586 Å with increasing Ti content (Table I). This indicates that the homogeneous solid solution phases were formed with Ti ions randomly occupying the B sites. The decreasing lattice parameter is due to the higher electronegativity and smaller radius of Ti^{4+} compared to Nb^{5+}.

The room-temperature Raman spectra of the samples are shown in Fig. 2. The Ti addition has a strong influence on the phonon line shapes. The phonon mode near 800 cm^{-1} splits into two modes, while the modes at 530 and 600 cm^{-1} merge at the enhanced Ti concentration. The low-frequency external mode near 50 cm^{-1} shifts to higher frequencies (blueshift) and finally merges with the mode near 95 cm^{-1}. Also the mode near 200 cm^{-1} exhibits a remarkable blueshift corresponding to a reduced unit cell size (see XRD data) at a higher Ti concentration. The substitution of Ti atoms into Zn or Nb sites causes a distortion of the Nb–O and Zn–O bonds, which leads to the splitting of the 800 cm^{-1} mode. This distortion is also linked to the unit cell shrinking. A blueshift of practically all phonon modes is seen also in IR reflectivity spectra (see Fig. 3 and Table II). Parameters of all observed polar modes are listed in Table II and one can see that the sum of dielectric contributions of all modes increases with Ti concentration. This result is consistent with the dielectric

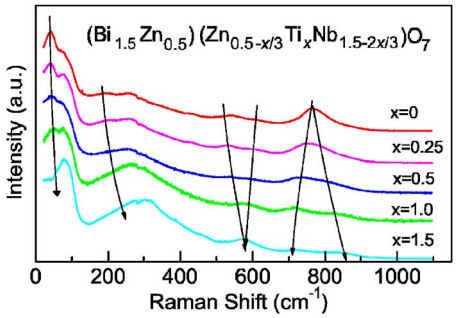

FIG. 2. (Color online) Room-temperature Raman spectra of $(Bi_{1.5}Zn_{0.5})\times(Zn_{0.5-x/3}Ti_xNb_{1.5-2x/3})O_7$ ceramics.

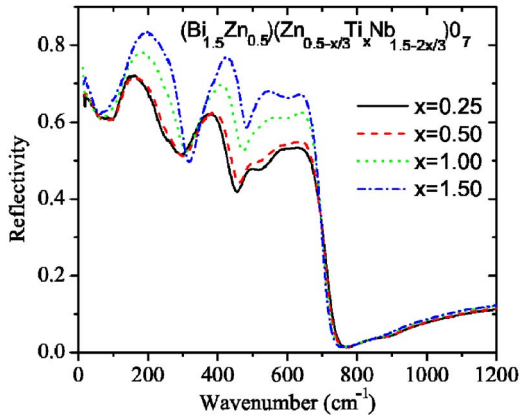

FIG. 3. (Color online) Room-temperature IR reflectivity spectra of $(Bi_{1.5}Zn_{0.5})(Zn_{0.5-x/3}Ti_xNb_{1.5-2x/3})O_7$ ceramics.

measurements. However, in our case, the low-frequency permittivity is determined not only by polar phonons but also by the contribution of the MW relaxation, which was roughly fitted to an overdamped ($\gamma_1 > 2\omega_1$) oscillator (will be discussed below). One can see from Table II and Fig. 7(a) that the phonon contributions to permittivity increase from 50 ($x=0.25$) to 70 ($x=1.5$), while the relaxation contribution from 99 ($x=0.25$) to 129 ($x=1.5$).

On cooling, the low temperature Raman spectra (not shown here) did not reveal any drastic changes, which indicates no structural changes down to low temperatures. The same behavior was observed earlier in low-temperature IR spectra of $Bi_{1.5}ZnNb_{1.5}O_7$.[18,24] The phonon peaks show only a small blueshift due to the thermal shrinking of the crystal lattice and a usual decrease of damping on cooling. We note that all polar phonons were assigned in Ref. 25 and the factor group analysis of lattice vibrations was published in Refs. 18 and 24.

The microwave dielectric properties of $(Bi_{1.5}Zn_{0.5})\times(Zn_{0.5-x/3}Ti_xNb_{1.5-2x/3})O_7$ ceramics are listed in Table I. The titanium doping gradually enhances the permittivity from 150 at $x=0.25$ to 200 at $x=1.5$ but shows surprisingly

TABLE II. Mode parameters of polar phonons in $(Bi_{1.5}Zn_{0.5})\times(Zn_{0.5-x/3}Ti_xNb_{1.5-2x/3})O_7$ ceramics in which first overdamped mode expresses the relaxation mode.

$x=0.25$, $\varepsilon_\infty=5.8$				$x=1.5$, $\varepsilon_\infty=6.5$			
No. of modes	ω_j (cm^{-1})	$\Delta\varepsilon_j$	γ_j (cm^{-1})	No. of modes	ω_j (cm^{-1})	$\Delta\varepsilon_j$	γ_j (cm^{-1})
1	42.3	99.3	238.2	1	31.4	128.8	113.0
2	138.2	1.2	19.2	2	162.5	37.1	36.8
3	150.3	29.0	60.7	3	182.7	14.9	49.3
4	186.2	1.8	42.2	4	220.9	3.6	81.7
5	211.6	0.5	35.7	5	246.3	1.5	70.5
6	259.0	5.7	139.1	6	362.0	5.1	62.2
7	312.2	0.1	32.2	7	395.5	1.6	48.3
8	346.9	4.61	92.7	8	505.4	1.2	78.6
9	483.4	0.9	73.3	9	592.1	0.5	116.1
10	522.7	0.04	38.5				
11	550.5	0.8	95.0				
12	608.3	0.3	117.8				

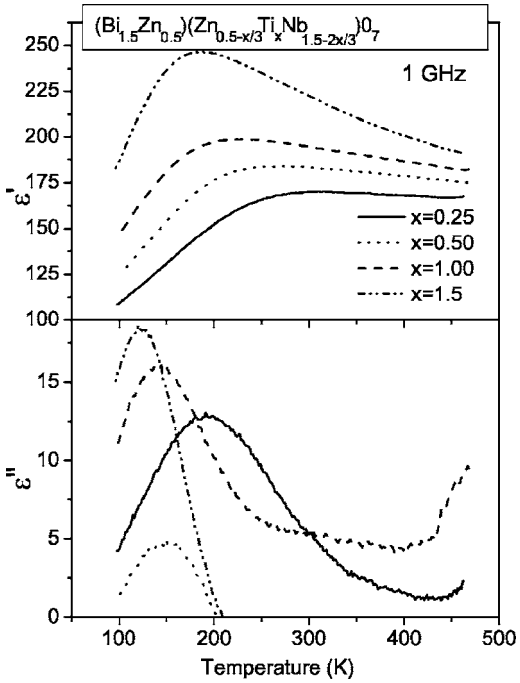

FIG. 4. Temperature dependence of real and imaginary parts of permittivity of $(Bi_{1.5}Zn_{0.5})(Zn_{0.5-x/3}Ti_xNb_{1.5-2x/3})O_7$ ceramics at 1 GHz.

no remarkable effect on the dielectric loss. It even seems that Q has a tendency to increase slightly with enhanced Ti concentration (i.e., permittivity). However, the temperature coefficient of resonance frequency τ_f increases with Ti content. The temperature dependences of the dielectric permittivity at 1 GHz for various doped ceramics are shown in Fig. 4. The curve of $x=0$ sample is almost identical with that of $x=0.25$; therefore it is not plotted in Fig. 4. All samples exhibit a decrease of permittivity at low temperatures and one can also see a gradual decrease of temperature of the permittivity maxima T_m with Ti concentration (this is discussed below).

Temperature and frequency dependences of the complex permittivity of $x=0.25$ and $x=1.5$ ceramics are shown in Figs. 5 and 6, respectively. The broad peaks of the real and imaginary parts of the complex permittivity $\varepsilon'(T)$ and $\varepsilon''(T)$ move towards higher temperatures on increasing frequency. A similar behavior is known from dipolar glass or relaxor ferroelectric systems.[26] Dielectric dispersion takes place in a broad temperature range both below and above T_m. For revealing the nature of the dielectric dispersion, it is better to consider the frequency spectra of the complex permittivity in Fig. 6. At high temperatures, the dielectric dispersion can be fitted to the Cole-Cole relaxation formula,

$$\varepsilon^*(\omega) = \varepsilon_\infty + \varepsilon^*_{\mathrm{ph}} + \frac{\Delta\varepsilon_R}{1+(i\omega\tau_R)^{1-\alpha}}, \tag{3}$$

where $\Delta\varepsilon_R$ and τ_R express the dielectric contribution of the relaxation to static permittivity and the mean relaxation time, respectively. α is the parameter expressing the distribution of relaxation frequencies ($0 \leqslant \alpha \leqslant 1$). The frequencies of dielectric loss $\varepsilon''(\omega)$ peaks correspond to mean relaxation frequencies $\omega_R = 2\pi/\tau_R$. Unfortunately, for our samples, ω_R lies mostly beyond our MW frequency limit; therefore it is not seen in Fig. 6. Nevertheless one can see that for a given temperature, e.g., 300 K, the low-frequency wing of the relaxation is better seen at $x=0.25$ than for the most doped sample; this means that ω_R increases with Ti doping. The same tendency was observed also in $x=0.5$ and $x=1.0$ ceramics (not shown here). The frequency ω_R corresponds to

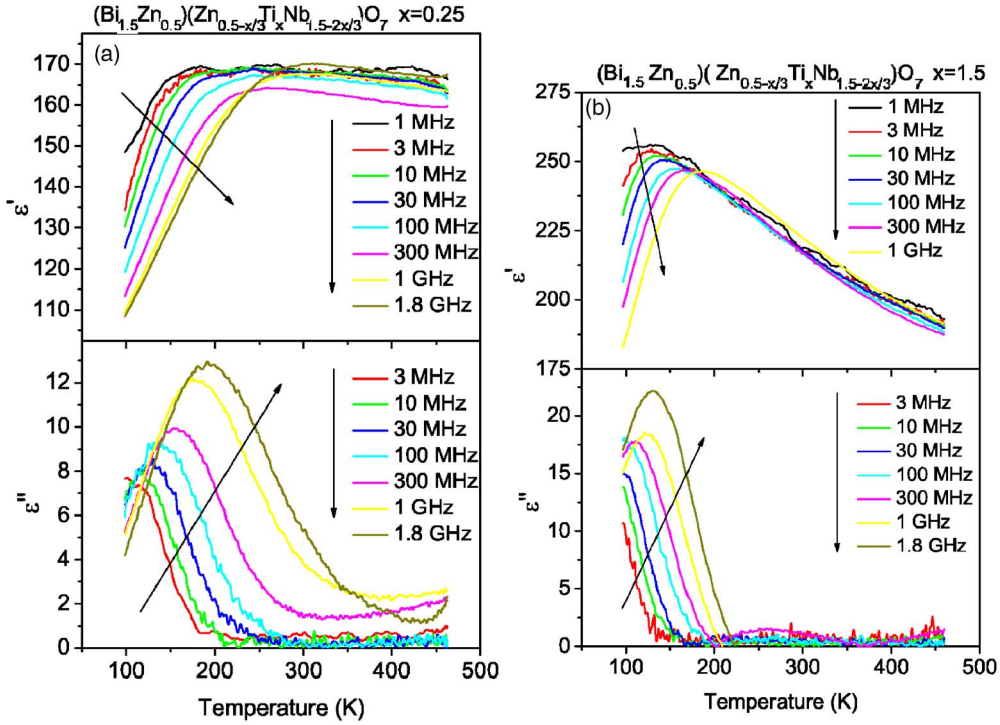

FIG. 5. (Color online) Temperature dependence of real and imaginary parts of permittivity of $x=0.25$ (a) and $x=1.5$ (b) $(Bi_{1.5}Zn_{0.5})\times(Zn_{0.5-x/3}Ti_xNb_{1.5-2x/3})O_7$ ceramics.

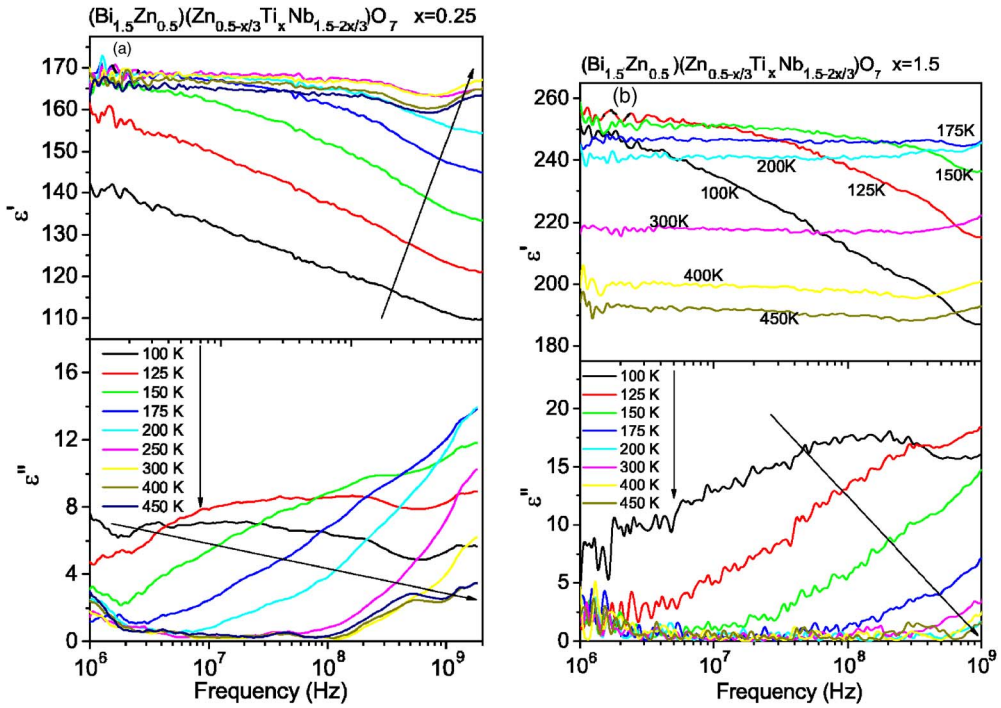

FIG. 6. (Color online) Frequency dependence of real and imaginary parts of permittivity of $x=0.25$ (a) and $(Bi_{1.5}Zn_{0.5})(Zn_{0.5-x/3}Ti_xNb_{1.5-2x/3})O_7$ ceramics.

the first maximum of dielectric loss spectra $\varepsilon''(\omega)$ which can be obtained from our overdamped oscillator fits as

$$\omega_R = \frac{\omega_1^2}{\gamma_1}, \tag{4}$$

where ω_1 and γ_1 are frequency and damping of the first polar mode, respectively (see Table II). In our case ω_R increases from 7.5 ($x=0.25$) to 8.7 cm^{-1} ($x=1.5$). The relaxation expresses the temperature activated hopping of disordered ions; therefore ω_R decreases on cooling and follows the Arrhenius dependence,

$$\omega_R = \omega_\infty \exp\left(\frac{-E_a}{kT}\right), \tag{5}$$

where ω_∞ denotes the relaxation frequency at infinite temperature, E_a is the activation energy, i.e., the hopping barrier height, k is the Boltzmann constant, and T is temperature. If at some temperature ω_R decreases below the measuring frequency, the relaxation does not contribute to the permittivity anymore and a decrease in $\varepsilon'(T)$ appears. Since ω_R is temperature dependent, the temperature of the decrease is frequency dependent. In our case we see the shift of T_m by about 100 K if the frequency changes by three orders of magnitude (see Fig. 5). It appears not only due to the Arrhenius law but also due to a very broad distribution of relaxation frequencies ($\alpha>0$). We did not fit the distribution of relaxation frequencies in our samples because of the lack of terahertz data below room temperature, but it is known from pure $(Bi_{1.5}Zn_{0.5})(Zn_{0.5}Nb_{1.5})O_7$ that the distribution of relaxation frequencies is extremely broad and widens with lowering temperatures.[18] This manifests itself in our samples by a very broad $\varepsilon''(\omega)$ loss peak at low T (see Fig. 6). An almost frequency-independent dielectric loss is seen for $x=0.25$ at 100 K. Similar spectra were observed in $(Bi_{1.5}Zn_{0.5})\times(Zn_{0.5}Nb_{1.5})O_7$ and fitted with a uniform distribution function of relaxation frequencies.[18]

The dielectric spectra in Fig. 6 (as well as the related shift down of T_m with increasing Ti concentration) give evidence of the rise of ω_R in the MW range with Ti concentration. This explains also a small increase of Q with x at room temperature (Table I), because if ω_R increases well above 2.5 GHz, the dielectric losses ε'' near 2.5 GHz decrease. The MW dielectric relaxation is also responsible for a much lower Q in cubic BZN pyrochlores than in the monoclinic one, which shows no MW relaxation.[19,27] Nevertheless, the MW relaxation has only a small influence on the dielectric losses at 1 MHz; therefore the Q at 1 MHz is comparable in both monoclinic and cubic BZN pyrochlores.[27]

As for the origin of the relaxation, it can stem from the hopping of dynamically disordered A and O' atoms among the possible sites. It is clear that the inhomogeneous distribution of Zn atoms and vacancies at the Bi sites gives rise to additional random fields. This could yield multiwell potentials for Zn and Bi cations at A sites that have a wide distribution of heights and therefore of transition rates for anharmonic hopping. A disorder of atoms at A sites together with associated structural relaxation of $O'A_2$ substructure was first proposed by Levin *et al.*[3] and recently it has been confirmed by direct transmission electron microscopy (TEM)

TABLE III. Fitting parameters of ω_∞ and E_a from Arrhenius equation (5).

x	T_m (°C) (1 GHz)	ω_∞	E_a (eV)
0.25	262.7	2.97×10^{12}	0.126
0.5	257.2	9.57×10^{12}	0.121
1.0	221.9	4.69×10^{12}	0.102
1.5	187.8	1.56×10^{13}	0.102

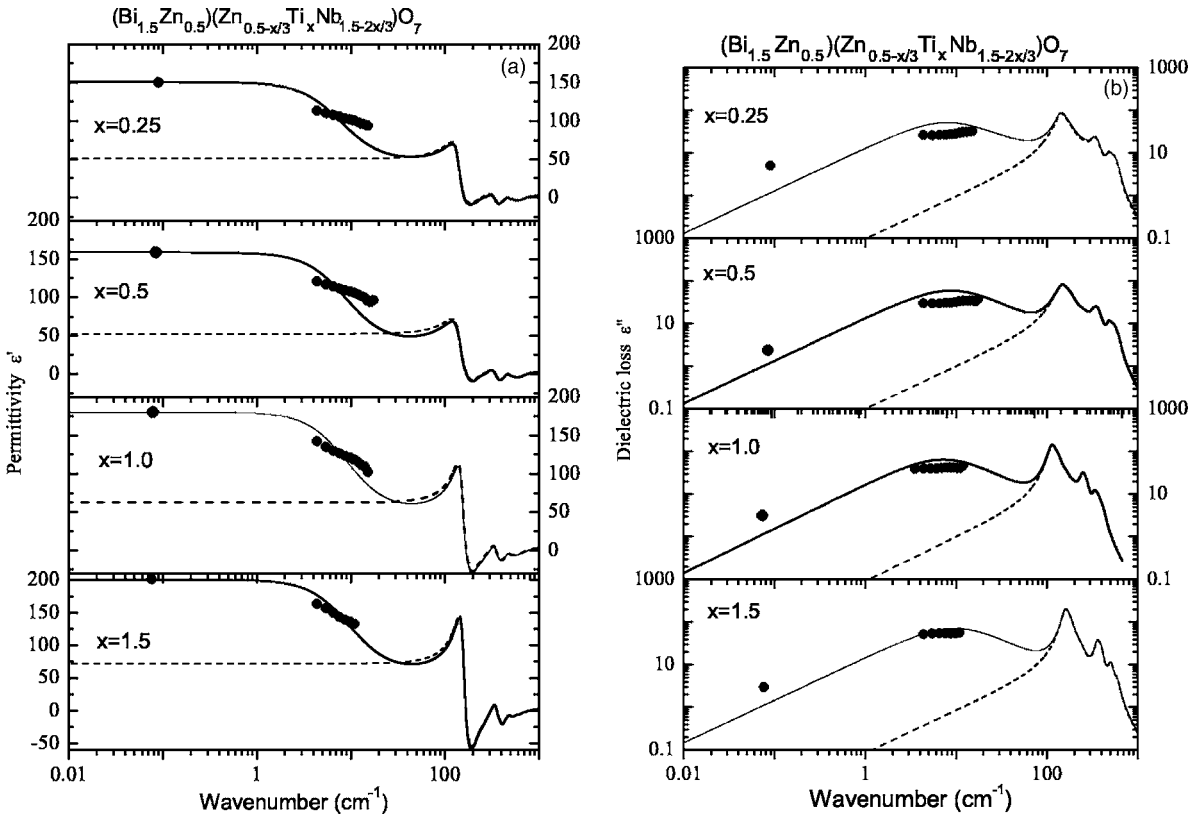

FIG. 7. Real (a) and imaginary (b) parts of complex dielectric spectra of $(Bi_{1.5}Zn_{0.5})(Zn_{0.5-x/3}Ti_xNb_{1.5-2x/3})O_7$ ceramics. Full symbols are experimental MW and terahertz data; solid lines are the results of the fits of IR and terahertz spectra. Dotted lines show only phonon contribution to complex permittivity.

observations.[28,29] It was also shown that such structural disorder is not affected by *B* site substitution of Nb ions by Ti or Sn ions.[29] The broad distribution of relaxation frequencies is caused by a distribution of activation energies for hopping of *A* and O′ atoms atoms from zero to about $E_a=0.2$ eV in pure $(Bi_{1.5}Zn_{0.5})(Zn_{0.5}Nb_{1.5})O_7$.[18] In the case of Ti containing samples, a similar broad relaxation was also observed and the upper limit for activation energies E_a decreases with Ti concentration. Table III shows E_a obtained from the fits of temperatures of dielectric loss maxima at various frequencies. It decreases from $E_a=0.126$ eV ($x=0.25$) down to 0.101 eV ($x=1.5$). Decrease of E_a with x explains also the observed increase of mean relaxation frequency with x.

Figure 7 shows the calculated permittivity $\varepsilon'(\omega)$ and loss $\varepsilon''(\omega)$ spectra obtained from our fits to experimental results based on the IR reflectivity, terahertz transmittance and MW data. An overdamped oscillator was used for a rough fit of dielectric relaxation below the phonon frequencies; however, this model is not very accurate because it does not express a broad distribution of relaxation frequencies. We tried to use also the Cole-Cole model, but the fit was not satisfactory. This model as well as a Debye relaxation model do not satisfy the sum rules; therefore these models deteriorate the fit of infrared reflectivity spectra. The model of uniform distribution of relaxation frequencies was used in Ref. 18 for the fit of wide dielectric spectra in pure $Bi_{1.5}ZnNb_{1.5}O_7$ and the same model could be in principle used also in our system, but it is beyond the scope of this paper. Figure 7 shows illustratively the phonon contribution to complex permittivity (dashed line). One can see that the phonon as well as relaxation contributions increase with Ti concentration. On the other hand, it is clear that the phonon (intrinsic) contribution to dielectric loss is much lower than the real experimental data [see Fig. 7(b)].

IV. CONCLUSION

Structure, MW dielectric relaxation and polar phonon modes of cubic pyrochlore $(Bi_{1.5}Zn_{0.5})\times(Zn_{0.5-x/3}Ti_xNb_{1.5-2x/3})O_7$ $(0\leqslant x\leqslant 1.5)$ ceramics were investigated. All the ceramics exhibit cubic pyrochlore structure. Ti substitution of *B* site atoms causes an increase of MW permittivity from 150 to 200 as well as a rise of MW relaxation frequency, which causes an increase of MW quality. The relaxation stems from the hopping of Bi and Zn atoms in the *A* sites and O′ atoms among several local potential minima. Disorder of these atoms is only slightly influenced by Ti substitution in the *B* sites; activation energy for hopping of disordered atoms decreases with x. MW permittivity increases with Ti substitution due to enhanced polar phonon and dielectric relaxation contributions. The rise of MW permittivity and quality with Ti concentration are promising for application of Ti substituted BZN ceramics in tunable MW devices.

ACKNOWLEDGMENTS

This work was supported by National 973-project of China under Grant No. 2002CB613302, NSFC project of China under Grant No. 50572085, Program for New Century Excellent Talents in University of China and Grant Agency

of the Czech Republic (Projects Nos. 202/04/0993 and AVOZ 10100520), and Academy of Sciences of the Czech Republic (Project No. A1010213).

[1]Z. P. Wang, S. Y. Zhang, Electronic Components & Materials **1**, 11 (1979).
[2]H. Wang, X. Wang, L. Zhang, and X. Yao, *Proceedings of the Fourth International Conference on Electronic Ceramics and Applications, Aachen, Germany 5–7 September 1994* (Augustinug Bachhandlung, Aachen, 1994), pp. 143–146.
[3]I. Levin, T. G. Amos, J. C. Nino, T. A. Vanderah, C. A. Randall, and M. T. Lanagan, J. Solid State Chem. **168**, 69 (2002).
[4]J. C. Nino, M. T. Lanagan, and C. A. Randall, J. Appl. Phys. **89**, 4512 (2001).
[5]X. Wang, H. Wang, and X. Yao, J. Am. Ceram. Soc. **80**, 2745 (1997).
[6]D. Liu, Y. Liu, S. Huang, and X. Yao, J. Am. Ceram. Soc. **76**, 2129 (1993).
[7]S. L. Swartz and T. R. Shrout, U.S. Patent No. 5,449,652 (12 September, 1995).
[8]W. Ren, S. Trolier-McKinstry, C. A. Randall, and T. R. Shrout, J. Appl. Phys. **89**, 767 (2001).
[9]R. L. Thayer, C. A. Randall, and S. Trolier-McKinstry, J. Appl. Phys. **94**, 1941 (2003).
[10]A. K. Tagantsev, J. Lu, and S. Stemmer, Appl. Phys. Lett. **86**, 032901 (2005).
[11]H. Wang, Ph.D. thesis, The Xi'an Jiaotong University, 1998.
[12]H. Wang and X. Yao, J. Mater. Res. **16**, 83 (2001).
[13]H. Wang, X. Wang, and X. Yao, Ferroelectrics **195**, 19 (1997).
[14]W. Zhang *et al.*, Proc. SPIE **4587**, 127 (2001).
[15]I.-D. Kim, Y.-W. Choi, and H. L. Tuller, Appl. Phys. Lett. **87**, 043509 (2005).
[16]X. Cai, L. Zhang, and X. Yao, Ferroelectrics **154**, 319 (1994).
[17]D. P. Cann, C. A. Randall, and T. R. Shrout, Solid State Commun. **100**, 529 (1996).
[18]S. Kamba *et al.*, Phys. Rev. B **66**, 054106 (2002).
[19]J. Petzelt and S. Kamba, Mater. Chem. Phys. **79**, 175 (2003).
[20]M. Valant and P. K. Davies, J. Am. Ceram. Soc. **83**, 147 (2000).
[21]M. Valant and P. K. Davies, J. Mater. Sci. **34**, 5437 (1999).
[22]H. Du and X. Yao, Physica B **324**, 121 (2002).
[23]H. Du and X. Yao, Mater. Res. Bull. **40**, 1527 (2005).
[24]M. Chen, D. B. Tanner, and J. C. Nino, Phys. Rev. B **72**, 054303 (2005).
[25]J. C. Nino, M. T. Lanagan, C. A. Randall, and S. Kamba, Appl. Phys. Lett. **81**, 4404 (2002).
[26]E. Buixaderas, S. Kamba, and J. Petzelt, Ferroelectrics **308**, 131 (2004).
[27]H. Wang, S. Kamba, M. Zhang, X. Yao, S. Denisov, F. Kadlec, and J. Petzelt, J. Appl. Phys. (to be published).
[28]R. L. Withers, T. R. Welberry, A.-K. Larsson, Y. Liu, L. Norén, H. Rundlöf, and F. J. Frank, J. Solid State Chem. **177**, 231 (2004).
[29]Y. Liu, R. L. Withers, T. R. Welberry, H. Wang, H. Du, and X. Yao, J. Electroceram. (to be published).